

# Critical Properties of the One-Dimensional Forest-Fire Model

A. Honecker and I. Peschel

*Fachbereich Physik, Freie Universität Berlin,  
Arnimallee 14, D-14195 Berlin, Germany*

## Abstract

A one-dimensional forest-fire model including lightnings is studied numerically and analytically. For the tree correlation function, a new correlation length with critical exponent  $\nu \approx 5/6$  is found by simulations. A Hamiltonian formulation is introduced which enables one to study the stationary state close to the critical point using quantum-mechanical perturbation theory. With this formulation also the structure of the low-lying relaxation spectrum and the critical behaviour of the smallest complex gap are investigated numerically. Finally, it is shown that critical correlation functions can be obtained from a simplified model involving only the total number of trees although such simplified models are unable to reproduce the correct off-critical behaviour.

---

e-mail:

honecker@omega.physik.fu-berlin.de  
peschel@aster.physik.fu-berlin.de

# 1. Introduction

---

Power laws and scaling behaviour, familiar from equilibrium critical phenomena, can also be found in non-equilibrium systems. If in such a case no fine-tuning of a parameter is necessary, the situation has been described as self-organized criticality [1, 2]. To illustrate the phenomenon, simple models for sandpiles [1, 2], forest fires [3] or evolution [4, 5] have been proposed. Their common feature are avalanche-type processes in the dynamics. In the case of the forest-fire models (ffm), the originally proposed version did not show proper scaling behaviour [6, 7], and it was necessary to introduce lightning strokes in order to find it [8]. Even then, the spatial power laws are valid only up to a typical length depending on the lightning rate. Therefore the ffm is in general not at a critical point, but only close to it. This is also the picture obtained from a renormalization treatment [9]. Nevertheless, the ffms are interesting systems (for a brief review see [10] and for a recent account [11]), and a detailed understanding of their properties, in particular in comparison with usual critical systems, is desirable. This should be simplest in the one-dimensional case.

In one dimension, a few exact results have been obtained [12, 13]. In particular, the stationary distribution of tree clusters with size  $s$  is given by [13]

$$n(s) = \frac{(1 - \rho)}{(s + 1)(s + 2)} \quad (1.1)$$

where  $\rho$  is the density. This expression is valid for  $s \ll \xi_c$  and gives  $n(s) \sim s^{-2}$  for large  $s$ . The length  $\xi_c$  depends on the rates  $p$  (for tree growth) and  $f$  (for lightning strokes) as  $\xi_c \sim p/f$ , up to logarithmic corrections. Thus, the corresponding exponent is  $\nu = 1$ . The time correlation function of burning trees could also be obtained. These results were checked by numerical calculations and an overall picture has emerged. However, the precise nature of the stationary state or the form of the relaxation spectrum are still to be determined.

To make some progress in this direction, we first studied the stationary correlations in more detail. In particular, we looked at the simple tree correlation function and found an unexpected result, namely a different correlation length which diverges with an exponent  $\nu_T \approx 5/6$ . This is in contrast to results in two dimensions [14] and indicates a rather complicated structure of the stationary state. To obtain this state explicitly, one has to treat the master equation. For this we used a quantum-mechanical formulation which has proved to be quite useful in other problems (see for example [15]). If one assumes instant burning of tree clusters, one then obtains a spin one-half quantum chain with both single and cluster-flip processes. A number of eigenstates can be found exactly, but in general one has to resort to numerics. We calculated the low-lying spectrum for systems up to  $L = 20$  sites, obtaining various branches in the complex plane and a gap which closes algebraically as the rate  $f$  goes to zero. We also considered the limit  $f \rightarrow 0$  analytically and found that to order  $\mathcal{O}(f)$  the ground state lies in a subspace of  $L + 1$  totally symmetric configurations. Working only in this subspace, one obtains a simple model where the system evolves in cycles [16]. Then the stationary state can be found explicitly and gives the cluster distribution (1.1) but it contains no correlations. Also the low-lying spectrum differs from the exact one. A similar observation for models of evolution has already been made in [17] where it was concluded that the behaviour of only one quantity is not a

sufficient criterion for criticality. To pursue this aspect further, we also investigated to what extent the cluster-size distribution of the full model for  $f > 0$  can be recovered in the symmetric subspace.

## 2. Simulations of correlation functions

---

This section presents results of simulations of two correlation functions. First, the two-point function of trees is studied and it is shown that the exponent of the corresponding correlation length is not an integer. By contrast, the correlation function inside a single cluster shows a critical behaviour which is consistent with the critical exponent of the cluster-size distribution  $n(s)$  eq. (1.1).

The ffm introduced in [3] is defined on a cubic lattice in  $d$  dimensions. Any site can have three states: It can be empty, or it can either be occupied by a green tree or a by a burning tree. The dynamics of the model was specified in [3] by the following parallel update rules from one timestep to the next: a) A burning tree becomes an empty site. b) A green tree becomes a burning tree if at least one of its nearest neighbours is burning. c) At an empty site a green tree grows with probability  $p$ . In order to obtain proper critical behaviour, the following rule was added in [8]: d) Every green tree can spontaneously be struck by lightning with probability  $f$  and thus become a burning tree even if no neighbour is burning.

Quantities of interest in this model are in particular the forest clusters, i.e. maximal connected sets of green trees. In one dimension a forest cluster is a string of green trees bounded by empty sites and its size  $s$  is just the number of trees.

The critical point of the above ffm, which has been studied as an example of self-organized criticality, arises at  $p \rightarrow 0$  and  $f/p \rightarrow 0$ . Keeping  $f/p$  fixed and taking  $p \rightarrow 0$  has the effect that once a cluster is struck by lightning it burns down before anything else happens. After redefining the time scale, the problem reduces to a two-state model where only empty sites ( $E$ ) and trees ( $T$ ) occur. The dynamics of this effective model is specified by the following parallel update rules:

- 1) At an empty site a tree grows with probability  $p$ .
- 2) A forest cluster of size  $s$  is struck by lightning with rate  $fs$  and all trees inside it become empty sites during one timestep.

Simulations have been carried out almost always with this reduced model (see e.g. [18, 14]). Below we will always think of this reduced version if we refer to ‘the forest-fire model’. We will restrict our attention to the one-dimensional version with periodic boundary conditions. The size of the lattice will be denoted by  $L$ .

First we have investigated two-point functions of trees  $\langle T_x T_{x+y} \rangle$  in one dimension. To this end we have performed simulations for  $0.0025 \leq p \leq 0.01$  in the range  $2 \cdot 10^{-5} \leq f/p \leq 2 \cdot 10^{-2}$ . The sizes of lattices ranged between  $L = 4000$  for large  $f$  and  $L = 500000$  for small  $f$ . One random initial condition with density  $\rho = \frac{1}{2}$  was chosen. Then  $t_0$  iterations were performed in order to equilibrate the system (usually  $t_0 = 3000$ , only for very small  $f$  one needs a few more iterations). After that  $\langle T_x T_{x+y} \rangle$  was determined every 100 timesteps from  $t_0$  to  $t_0 + 1900$  by averaging over all  $x$ . This determination of  $\langle T_x T_{x+y} \rangle$  is much more time consuming than the simulation itself. The procedure was repeated 10 times with the same initial conditions, amounting to a total of  $200L$  measurements for  $\langle T_x T_{x+y} \rangle$ .

The resulting data can nicely be fitted by

$$C(y) := \langle T_x T_{x+y} \rangle - \langle T_x \rangle^2 = a e^{-y/\xi} \quad (2.1)$$

for  $1 \leq y$ . (Note that  $\langle T_x \rangle = \rho$  and  $T_x^2 = T_x$ .) The parameters  $a$  and  $\xi$  were estimated by taking the logarithm of the r.h.s. of (2.1) and then performing a linear regression for  $1 \leq y \leq y_{\max}$ .  $y_{\max}$  was chosen such that statistical errors can be neglected for  $y < y_{\max}$ . With the statistics of our simulations  $y_{\max}$  was always a few correlation lengths.

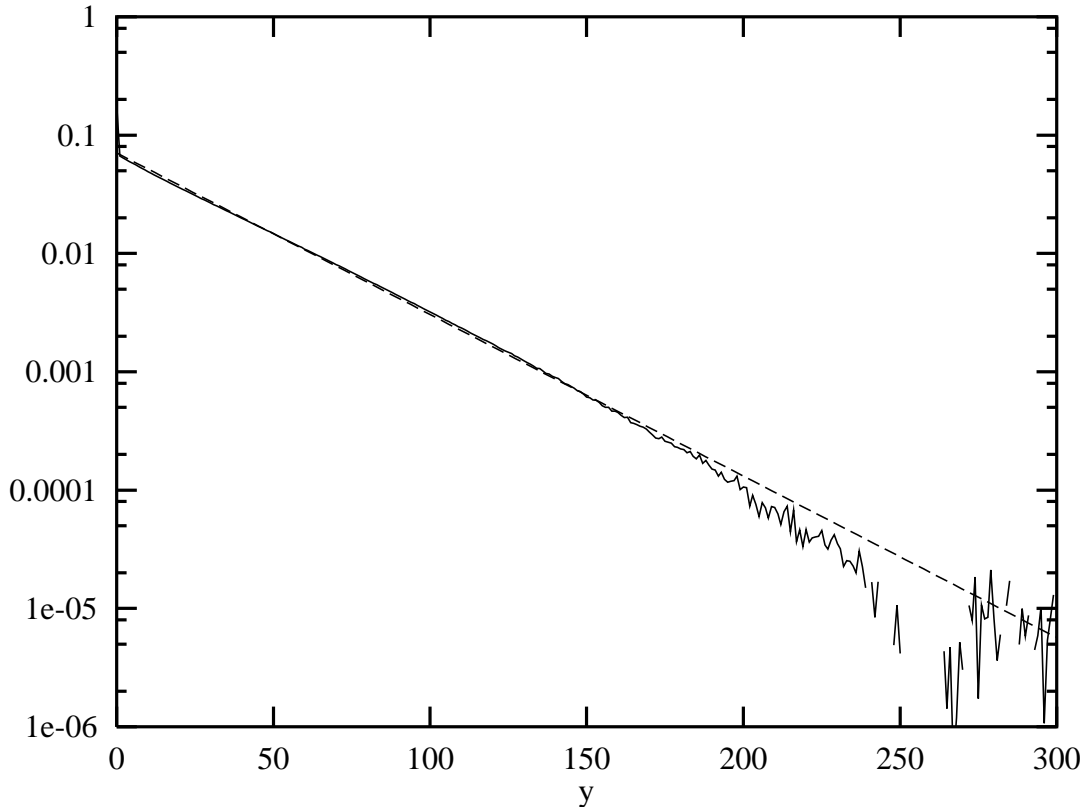


**Fig. 1:** The correlation function  $C(y)$  for  $L = 100000$ ,  $p = 1/200$ ,  $f/p = 1/100$  (full line). The dashed line is the exponential form (2.1) with  $a = 0.0707$ ,  $\xi = 31.81$ .

Fig. 1 shows the result of a detailed simulation where the average was taken every 100 timesteps over the larger time interval from  $t_0 = 3000$  to  $t_0 + 39900$ . The agreement of the simulation with the exponential form is very good for a few correlation lengths. For  $y \approx 200$  statistical errors start to become so large that the difference on the l.h.s. of (2.1) cannot be determined sufficiently accurately any more. For smaller values of  $y$  there are small wiggles over longer ranges of the distance  $y$  which are typical for the simulations and seem to be caused by statistical fluctuations. Apart from that, no substantial corrections to the form (2.1) are visible.

Fig. 2 shows the results of the correlation length  $\xi$  obtained from simulations as a function of  $f/p$ . There are some residual statistical as well as systematic errors due to a small  $p$ -dependence which are, however, not larger than the symbols. One can see that the values

for  $\xi$  (and similarly for  $a$ ) are in good agreement with the form

$$\xi \sim \left(\frac{f}{p}\right)^{-\nu_T}, \quad a \sim \left(\frac{f}{p}\right)^\mu. \quad (2.2)$$

Performing linear regression fits on a doubly logarithmic scale one finds

$$\nu_T = 0.8336 \pm 0.0036, \quad \mu = 0.1031 \pm 0.0022. \quad (2.3)$$

Surprisingly  $\nu_T$  agrees very well with the gap index  $\nu = 5/6$  for the three-state Potts model in two dimensions and its associated one-dimensional quantum chain [19]. The most probable rational value for the other exponent is  $\mu = 1/10$ .

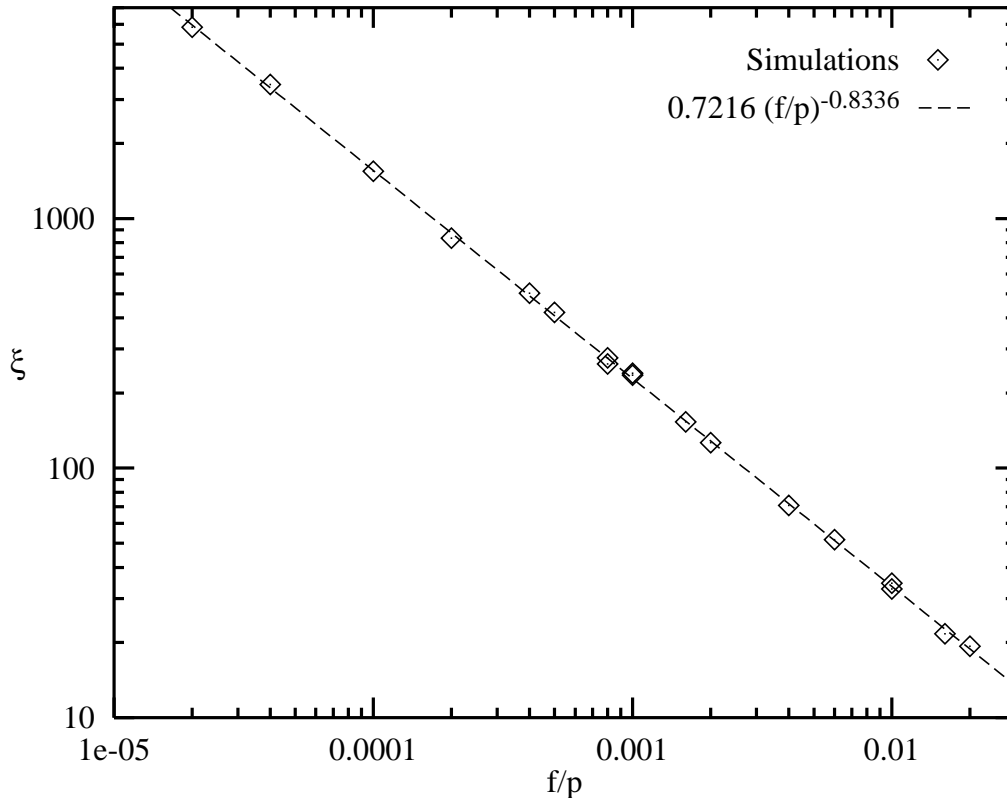


**Fig. 2:** The correlation length  $\xi$  as a function of  $f/p$  for various values of  $f$ ,  $p$  and  $L$ .

It was argued in [14] for two dimensions that the critical exponents are independent of the particular correlation function considered. In order to investigate this question in one dimension we also looked at the correlation function  $\langle T_x T_{x+y} \rangle_c$  describing the probability to find two trees at positions  $x$  and  $x + y$  *inside the same cluster*. In  $d = 1$  one has

$$\langle T_x T_{x+y} \rangle_c = \langle T_x T_{x+1} \dots T_{x+y} \rangle =: K(y). \quad (2.4)$$

This quantity can easily be simulated as before. Its determination is actually much less time consuming.

The correlation function  $K(y)$  can be fitted with a single exponential function for  $y$  sufficiently large, but for smaller  $y$  an exponential function is not a good approximation. Thus, we fit  $K(y)$  by

$$K(y) = \sum_{r=1}^{\infty} a^{(r)} e^{-y/\xi_c^{(r)}} \quad (2.5)$$

where the  $\xi_c^{(r)}$  decrease with  $r$ . The first few terms in the sum (2.5) already give excellent approximations. In an interval  $y_{\min} \leq y \leq y_{\max}$  all terms with  $r > 1$  can be neglected and this can be used to estimate the largest decay length  $\xi_c = \xi_c^{(1)}$  with a linear regression for the logarithm of the correlation function  $K(y)$ . Typically one finds  $y_{\min} \approx \xi_c$ ,  $y_{\max} \geq 5\xi_c$ .

Note that  $K(y)$  is related to the cluster-size distribution  $n(s)$  via

$$K(y) = \sum_{s>y} (s-y)n(s). \quad (2.6)$$

This can be inverted to give

$$n(s) = K(s-1) - 2K(s) + K(s+1). \quad (2.7)$$

This implies that if  $K(s)$  decays exponentially in some region, also  $n(s)$  must decay exponentially in roughly the same region. However, the lattice Laplacian in (2.7) increases the weight of the next to leading terms in (2.5). Therefore, the purely exponential decay is expected to set in at larger  $s$  for  $n(s)$  than for  $K(s)$ . The value  $s_0$  where a single exponential function starts to describe  $n(s)$  can be estimated as follows. One requires that the form  $n(s) = (1-\rho)/s^2$  can be matched up to the linear term at  $s_0$  with a single exponential function for  $K(s)$ , i.e.  $K(s) = ae^{-s/\xi_c}$ . According to (2.7) one must have  $n(s_0) = \frac{\partial^2}{\partial s^2} K(s)|_{s=s_0}$  and  $\frac{\partial}{\partial s} n(s)|_{s=s_0} = \frac{\partial^3}{\partial s^3} K(s)|_{s=s_0}$ . This leads to the relation  $a \approx (1-\rho)$  (which is indeed well verified in simulations) for the normalization constants and  $s_0 \approx \xi_c$  for the desired crossover point.

Fig. 3 shows the correlation function  $K(s)$  and the normalized cluster-size distribution  $n(s)$ . The simulation was performed in the same manner as in Fig. 1.  $n(s)$  was determined by counting all clusters of size  $s$  in the system during each of the 40000 timesteps after  $t_0 = 3000$ . In this time-interval, estimates for  $K(y)$  were obtained every hundredth timestep as a spatial average over the entire system. The huge amount of data in particular for  $n(s)$  is needed in order to obtain small statistical fluctuations without too much extra smoothing. One observes that both expectation values decay exponentially over a large range of  $s$ . The correlation lengths obtained by fits in this region agree very well with each other as it should be according to (2.7). The actual value is  $\xi_c \approx 28$ . Furthermore, the crossover of the cluster-size distribution from the form (1.1) to the exponential decay does indeed occur in the vicinity of one correlation length, the exponential decay being well visible beyond  $s = 10\xi_c$ . It seems that  $K(y)$  starts to decay faster than exponentially around  $s = 400$  in Fig. 3. However, comparison with simulations with a smaller amount of samples indicates that this effect is a residual statistical error. Thus, the exponential decay of  $n(s)$  and  $K(s)$  could well extend indefinitely, the probability of clusters larger than 450 trees simply being so small that they did not appear in the present simulation.

Although the simulation in Fig. 3 was performed for a fairly large value of  $f/p$ , it does reflect the typical situation also closer to the critical point  $f/p = 0$ . The form (1.1) for  $n(s)$  is valid approximately up to one correlation length  $\xi_c$ , while the exponential decay can be verified for at least a few  $\xi_c$ . For smaller  $f/p$  than in Fig. 3 there is a small difference: There is a region where the form (1.1) for  $n(s)$  lies below the actual exponential decrease. This corresponds to the ‘bump’ observed in a logarithmic plot of the cluster size distribution [13].

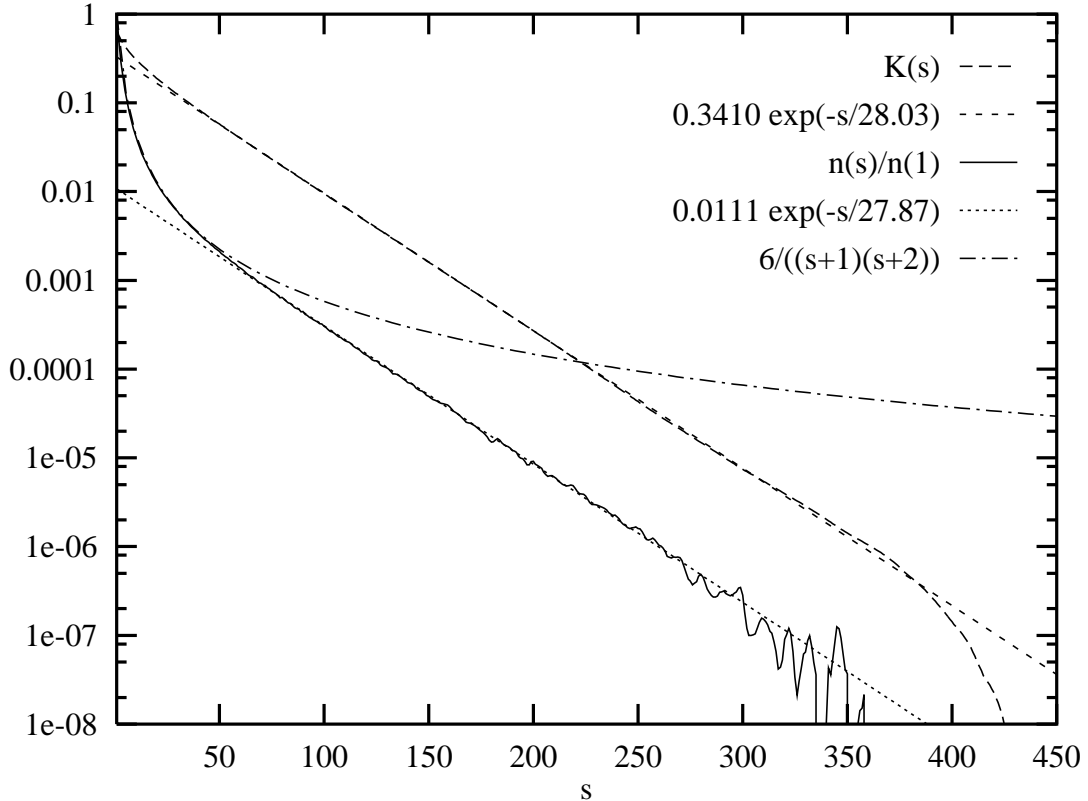


**Fig. 3:** The correlation function  $K(s)$  and the cluster-size distribution  $n(s)$  for  $L = 100000$ ,  $p = 1/200$ ,  $f/p = 1/100$ .

There is a striking similarity of  $n(s)$  in Fig. 3 with the avalanche distribution shown in Fig. 6b of [20] for a different two-dimensional forest-fire model. This similarity might indicate that one could expect similar results for the two-dimensional version of the forest fire model considered in this paper, but it may also just illustrate the fact that cluster size distributions of very different models can qualitatively resemble each other.

We have also performed simulations to study the  $f/p$ -dependence of  $K(y)$ . They were done for  $4 \cdot 10^{-4} \leq f/p \leq 2 \cdot 10^{-2}$  and  $15000 \leq L \leq 500000$ . One finds that the resulting data is consistent with

$$\xi_c \ln(\xi_c) = (0.95 \pm 0.06) \frac{p}{f}. \quad (2.8)$$

The functional form of the relation (2.8) was already given in Ref. [13] although the derivation has to be considered with some care (see section 5 below).

This result is to be contrasted with the one for the two-point correlation function  $C(y)$ . The two-point function is significantly more accurately described by a single exponential

function (compare Figs. 1 and 3). Even more, the critical exponents are clearly different – see eq. (2.3). Thus, in one dimension there seems to be no direct relation between the two different correlation functions. Note that the relative errors in Ref. [14] for the critical exponents in two dimensions are much larger than the ones of our simulations. Therefore it is conceivable that a more precise study could reveal different exponents in two dimensions as well.

Finally, we would like to mention that an exponential decay of  $n(s)$  as found above, can already be obtained from a mean-field approximation. Complete factorization of the correlator defining  $n(s)$  yields  $n(s) = (1 - \rho)^2 \rho^s$ , i.e.  $n(s)$  varies exponentially. In the mean-field approximation for the original version of the ffm with burning trees one finds the critical behaviour  $1 - \rho \sim f/p$ . This implies  $\xi_c = -1/\ln(\rho) \sim p/f$ , i.e. the critical exponent is  $\nu = 1$  in mean-field approximation. This agrees with (2.8) up to logarithmic corrections but one should note that the critical behaviour of  $\rho$  is not right. The correct result is  $\rho/(1 - \rho) \sim \ln(p/f)$  [13] and the corresponding exponent differs by one from the mean-field result.

### 3. Hamiltonian formulation of the model

---

In this section we present a quantum-mechanical formulation of the ffm and use it to discuss correlations at the critical point.

In order to set up notations, let us briefly recall the Hamiltonian formulation of stochastic lattice models (see e.g. [15]). Denote the probability to find the system in a configuration  $\{\beta\}$  by  $P(\{\beta\})$ . Then the time evolution of the system is given by the master equation

$$\partial_t P(\{\beta\}) = - \sum_{\{\beta'\}} W_{\{\beta\} \rightarrow \{\beta'\}} P(\{\beta\}) + \sum_{\{\beta'\}} W_{\{\beta'\} \rightarrow \{\beta\}} P(\{\beta'\}) \quad (3.1)$$

where the two terms on the r.h.s. represent the loss and gain processes respectively. The symbol  $\partial_t$  can equally well denote evolution in discrete or continuous time. To formulate (3.1) in quantum-mechanical terms one introduces a basis of states  $|\{\beta\}\rangle$  corresponding to the configurations  $\{\beta\}$  and specifies the state of the system by a vector

$$|P\rangle = \sum_{\{\beta\}} P(\{\beta\}) |\{\beta\}\rangle. \quad (3.2)$$

Then the master equation (3.1) takes the form of a Schrödinger equation in imaginary time

$$\partial_t |P\rangle = -H |P\rangle \quad (3.3)$$

where the Hamiltonian  $H$  for a stochastic system is in general non-hermitean. Due to probability conservation one always has an eigenstate of  $H$  with eigenvalue zero.

In order to apply this general formalism to the ffm we choose the following basis at each site:

$$\begin{pmatrix} 0 \\ 1 \end{pmatrix} = \text{empty place} = 0, \quad \begin{pmatrix} 1 \\ 0 \end{pmatrix} = \text{tree} = 1. \quad (3.4)$$



The notation 0 and 1 corresponds to spin down ( $-1$ ) and spin up ( $+1$ ) in the usual spin language. A general state  $|\{\beta\}\rangle$  corresponding to a configuration of the complete system is given by

$$|\{\beta\}\rangle = |i_1 \dots i_L\rangle, \quad (3.5)$$

where  $i_x = 0, 1$  encodes the state of the site  $x$ . The vectors (3.5) form a basis of a  $2^L$  dimensional complex vector space. The notation  $T_x$  and  $E_x$  will be used for the operators that measure if site  $x$  is occupied by a tree or empty.

We will consider the case of small  $p$  and  $f$ . Then in each time step changes occur essentially only at one site and one can replace parallel dynamics by sequential dynamics. Note that for the original three-state model parallel dynamics is essential because e.g. the probability of fire spreading simultaneously at different places is large. With sequential dynamics the Hamiltonian takes the form

$$H = p H_0 + f V \quad (3.6a)$$

and can be written down explicitly using Pauli matrices. In terms of Pauli matrices the operators  $T_x$  and  $E_x$  are given by  $T_x = \frac{1}{2}(\mathbb{1} + \sigma^z)_x$  and  $E_x = \frac{1}{2}(\mathbb{1} - \sigma^z)_x$ . The state of a given site is changed by the operators  $\sigma^{\pm} = \frac{1}{2}(\sigma^x \pm i\sigma^y)$ .

$H_0$  is a sum of single-site terms  $(H_0)_x$  describing growth of a tree at site  $x$ . In spin language, the gain term then involves single spin flips from 0 to 1:

$$H_0 = \sum_{x=1}^L \left( \frac{1}{2}(\mathbb{1} - \sigma^z)_x - \sigma_x^+ \right). \quad (3.6b)$$

The term  $V$  describes the burning down of tree clusters and is given by

$$V = \sum_{x=1}^L \sum_{l=1}^L l \left\{ \frac{1}{2}(\mathbb{1} - \sigma^z)_x \frac{1}{2}(\mathbb{1} + \sigma^z)_{x+1} \cdots \frac{1}{2}(\mathbb{1} + \sigma^z)_{x+l} \frac{1}{2}(\mathbb{1} - \sigma^z)_{x+l+1} \right. \\ \left. - \frac{1}{2}(\mathbb{1} - \sigma^z)_x \sigma_{x+1}^- \cdots \sigma_{x+l}^- \frac{1}{2}(\mathbb{1} - \sigma^z)_{x+l+1} \right\} \quad (3.6c)$$

with suitable conventions such that the projectors at the boundary drop out for a cluster that occupies the entire system. This term contains flips of entire clusters from state 1 to the empty state 0. The weight of such a cluster-flip process is proportional to the size  $l$  of the cluster.

We would like to note that our Hamiltonian (3.6) is different from the one presented in Anhang B of [21]. Also the Fock space formulations of the master equation in [22, 23] are different since they treat situations with more than two states per site.

Clearly, it is possible to choose  $p = 1$  in (3.6a) by suitably rescaling  $H$ . Below we will assume  $p = 1$  and we will be interested in small  $f$ . Then one can apply standard quantum-mechanical perturbation theory to (3.6).

Before performing any computation one can already see that if one wants to take the limit  $L \rightarrow \infty$  of a perturbation expansion, one is forced to approach the critical point  $f = 0$ . This is due to the fact that a perturbation series is expected to converge as long as  $f$  times

the largest matrix element of  $V$  (which has value  $L$ ) is small compared to the distance 1 between the eigenvalues of  $H_0$ . This amounts to imposing

$$f L \ll 1 \quad (3.7)$$

in order to be on safe grounds. Thus, one is forced to let  $f \rightarrow 0$  as  $L \rightarrow \infty$ . In other words, the radius of convergence of the perturbation series is expected to be zero for  $L = \infty$ . Still, perturbation theory will tell us something about the properties of the critical point itself.

First, we use the Hamiltonian formulation of the ffm in order to determine the stationary state perturbatively. In order to simplify the presentation we introduce the notation

$$|N\rangle := \sum_{N \text{ empty places}} | \underbrace{01\dots} \rangle \quad (3.8)$$

for a sum over all configurations with a total of  $N$  empty places. For the stationary state  $|G\rangle$  perturbation theory is particularly simple. One makes the power-series ansatz  $|G\rangle = \sum_{\nu=0}^{\infty} f^{\nu} |G_{\nu}\rangle$ . Obviously  $|G_0\rangle = |1\dots 1\rangle = |0\rangle$ . For the first-order correction  $|G_1\rangle$ , the standard quantum-mechanical formulas lead to the condition  $H_0 |G_1\rangle + V |G_0\rangle = 0$  where the projection onto  $|G_0\rangle$  has to be subtracted. Since  $H_0$  as well as  $V |G_0\rangle$  are invariant under permutations of the spins,  $|G_1\rangle$  must also have this property and thus can be written as a superposition of the states  $|N\rangle$

$$|G_1\rangle = \sum_{N=1}^L \alpha_N |N\rangle. \quad (3.9)$$

Let us note that, apart from the growth processes, only one lightning process enters in this first-order calculation, namely the one leading from the completely full system to a completely empty system.

Using now that the coefficient of a state  $|N\rangle$  with  $1 \leq N \leq L-1$  in the expression for  $H_0 |G_1\rangle$  must be zero, one finds the recurrence relation  $\alpha_{N+1} = N/(L-N) \alpha_N$  for  $1 \leq N$ . The only further condition is  $\alpha_L = 1$ . This gives  $\alpha_N = \binom{L-1}{N-1}^{-1}$ . In summary, we have found that

$$|G\rangle = |1\dots 1\rangle + f \sum_{N=1}^L \frac{1}{\binom{L-1}{N-1}} |N\rangle + \mathcal{O}(f^2) \quad (3.10)$$

satisfies  $H |G\rangle = \mathcal{O}(f^2)$ .

Eq. (3.10) is in the form that arises naturally from perturbation theory, but is not yet properly normalized as a probability. Thus, we multiply the state  $|G\rangle$  with  $\mathcal{N}_L$  and impose the normalization condition that the sum of all coefficients in the state  $\mathcal{N}_L |G\rangle$  is one. This leads to

$$\frac{1}{\mathcal{N}_L} = 1 + f \sum_{N=1}^L \frac{\binom{L}{N}}{\binom{L-1}{N-1}} + \mathcal{O}(f^2) = 1 + fL \sum_{N=1}^L \frac{1}{N} + \mathcal{O}(f^2). \quad (3.11)$$

From (3.10) one can compute every correlation function for  $f \rightarrow 0$ . Let

$$n_r(s) = \langle E_{x_1} \dots E_{x_{r+1}} T_{x_{r+2}} \dots T_{x_{s+r+1}} \rangle \quad (3.12)$$

be any correlation function with  $s$  trees and  $r + 1$  empty places at certain fixed sites. Since (3.10) is invariant under a permutation of the  $L$  sites of the lattice, this correlation function will only depend on the total number of trees and empty places, respectively. From (3.10) one finds that

$$n_r(s) = \mathcal{N}_L f \sum_{N=r+1}^{L-s} \frac{\binom{L-s-r-1}{N-r-1}}{\binom{L-1}{N-1}} = \frac{\mathcal{N}_L f L r!}{(s+1)(s+2)\cdots(s+r+1)} \quad (3.13)$$

for any *finite* system,  $r \geq 0$  and  $0 \leq s \leq L - r - 1$ . The second identity is a purely combinatorial one and proven in appendix A for  $r = 0$ . For  $r > 0$  the result follows most easily from the equation of motion for  $n_r(s)$  in the stationary state (compare section 5). Note that any correlation function involving at least one empty place decays algebraically in this approximation, the chain length  $L$  acting as cutoff. Furthermore, tree-tree or cluster-cluster correlation functions are trivial in the sense that they do not depend on the distance between the trees, respective clusters.

Let us briefly comment on a few special cases of (3.13):

- 1) For the cluster-size distribution  $n(s) = n_1(s)$  one recovers the result (1.1) with  $1 - \rho = \mathcal{N}_L f L$ . A derivation of this result for  $r = 1$  along similar lines as above and in section 5 below can also be found in [13, 16]. In fact, the discussion of the stationary state at small  $f$  in [13] inspired us to apply quantum-mechanical perturbation theory to the ffm.
- 2) The probability to find a cluster of  $s$  empty places with two adjacent trees is given by  $n_{s-1}(2) = 2\mathcal{N}_L f L / (s(s+1)(s+2))$ . The functional form of this correlation function was already derived in [12]. Note that in eq. (5) of [12] which was used to obtain this result, the loss terms by a lightning stroke at the boundaries are missing. This is, however, irrelevant for the derivation of the form of  $n_{s-1}(2)$ .
- 3) For the probability to find a string of  $s$  adjacent empty sites one finds that  $n_{s-1}(0) = \mathcal{N}_L f L / s$  for  $1 \leq s \leq L - 1$ . For this special case it is also comparably easy to directly prove the combinatorial identity (3.13) by induction on  $L$ .
- 4) The probability  $K(s)$  to find  $s$  trees at certain places and *no* empty places can be obtained from (2.7) using (3.13) for  $n(s)$ . One finds in particular that  $K(s) \sim \ln(s)$  for large  $s$ . Note that the smaller the exponent of a correlation function the sooner will it be dominated by an exponential decay for  $f \neq 0$ . In particular, the asymptotic logarithmic behaviour of  $K(s)$  is therefore not observable in simulations (compare Fig. 3 of section 2).

It is also straightforward to compute the mean density of trees  $\rho$ . One finds that  $\rho / (1 - \rho) \sim \ln(L)$  for  $L$  large. This also shows that in this first-order approximation only the finite size of the system prevents it from being critical.

We now proceed with a discussion of the relaxation spectrum. For  $f = 0$  the operator  $H = H_0$  has real eigenvalues which are simple integers  $\Lambda = 0, 1, \dots, L$ . In general, one can use the fact that for periodic boundary conditions the lattice translation operator commutes with the Hamiltonian and the spectrum splits into  $L$  sectors with different momenta  $P$ . We introduce the notation

$$||i_1 i_2 \dots i_{L-1} i_L \rangle\rangle_P := |i_1 i_2 \dots i_{L-1} i_L \rangle + e^{iP} |i_L i_1 i_2 \dots \rangle + \dots + e^{i(L-1)P} |i_2 \dots i_{L-1} i_L i_1 \rangle \quad (3.14)$$

for states of fixed momentum  $P = 2\pi n/L$  and specify the first Brillouin zone by  $0 \leq n < L$ ,  $n \in \mathbb{Z}$ .

Some of the excited states can easily be written down. Using that a sum of all  $L$ th roots of unity vanishes, one can see that

$$\begin{aligned} H|01\dots 1\rangle_P &= (1 + f(L-1))|01\dots 1\rangle_P \\ H|001\dots 1\rangle_P &= (2 + f(L-2))|001\dots 1\rangle_P + (1 + e^{iP})|01\dots 1\rangle_P \end{aligned} \quad (3.15)$$

for  $P \neq 0$ . Eq. (3.15) implies that there are *exact* excited states with eigenvalue  $1 + f(L-1)$  and  $2 + f(L-2)$  respectively. However, for  $L$  large they will not belong to the low-lying part of the excitation spectrum.

Other excited states can be treated with standard quantum-mechanical perturbation theory, bearing in mind that the left and right eigenvectors have to be treated separately. Some computations are presented in appendix B. The final result for the states with eigenvalue  $\Lambda = 1$  of  $H_0$  is that  $H$  has  $L-1$  times the eigenvalue  $1 + f(L-1) + \mathcal{O}(f^2)$  and one times the eigenvalue  $1 + f(2L-1) + \mathcal{O}(f^2)$ . Similarly, the states with eigenvalue  $\Lambda = 2$  of  $H_0$  give rise to an eigenvalue  $2 + f(L-2) + \mathcal{O}(f^2)$  of  $H$  for each momentum (including the translationally invariant sector). In the translationally invariant sector this eigenvalue  $2 + f(L-2) + \mathcal{O}(f^2)$  can cross with the eigenvalue  $1 + f(2L-1) + \mathcal{O}(f^2)$  around  $f = 1/(L+1)$ . The physically interesting region is located beyond this crossing where the lowest eigenvalues form a complex-conjugate pair. However, there are fundamental obstacles to reach this region beyond the crossing with perturbation expansions around  $f = 0$ .

## 4. Numerical computation of the relaxation spectrum

In order to obtain results for the thermodynamic limit of the relaxation spectrum, one has to resort to a numerical diagonalization of the Hamiltonian at finite  $L$ . In this section we argue on the basis of such computations that the fermion has a non-vanishing complex gap in the thermodynamic limit for  $f > 0$ . The exponents describing the critical behaviour for  $f \rightarrow 0$  of the real and imaginary parts of this complex gap are both non-integral.

After projecting onto the eigenspaces (3.14) with fixed momentum  $P$ , the Hamiltonian (3.6) becomes a square matrix of approximate size  $2^L/L$ . Up to  $L = 20$ , where the size of the matrix is slightly larger than 50000, a few extremal eigenvalues can be obtained using standard methods.

In addition to translational invariance, the model is invariant under parity  $x \mapsto -x$ . This can be exploited to reduce the dimensionality of the problem a little further for  $P = 0$  and  $P = \pi$ . More important are the following consequences of the invariance with respect to parity:

- 1) The spectra in the sectors with momenta  $P$  and  $2\pi - P$  are equal.
- 2) In each sector with fixed momentum, the eigenvalues are either real or come in complex conjugate pairs. This holds because the characteristic polynomial of the complete Hamiltonian (3.6) is real, and because of property 1).

Fig. 4 shows the low-lying excitations  $\Lambda$  for  $L = 20$  and  $f = 0.1$  in the complex plane (the picture for  $L = 16$  is qualitatively similar). Because of the symmetries mentioned above

we have restricted ourselves to  $0 \leq P \leq \pi$  and to  $\text{Im}(\Lambda) \geq 0$ . Note that the figure does not include the ground state  $\Lambda = 0$  and that there are many more eigenvalues near its right end and beyond.

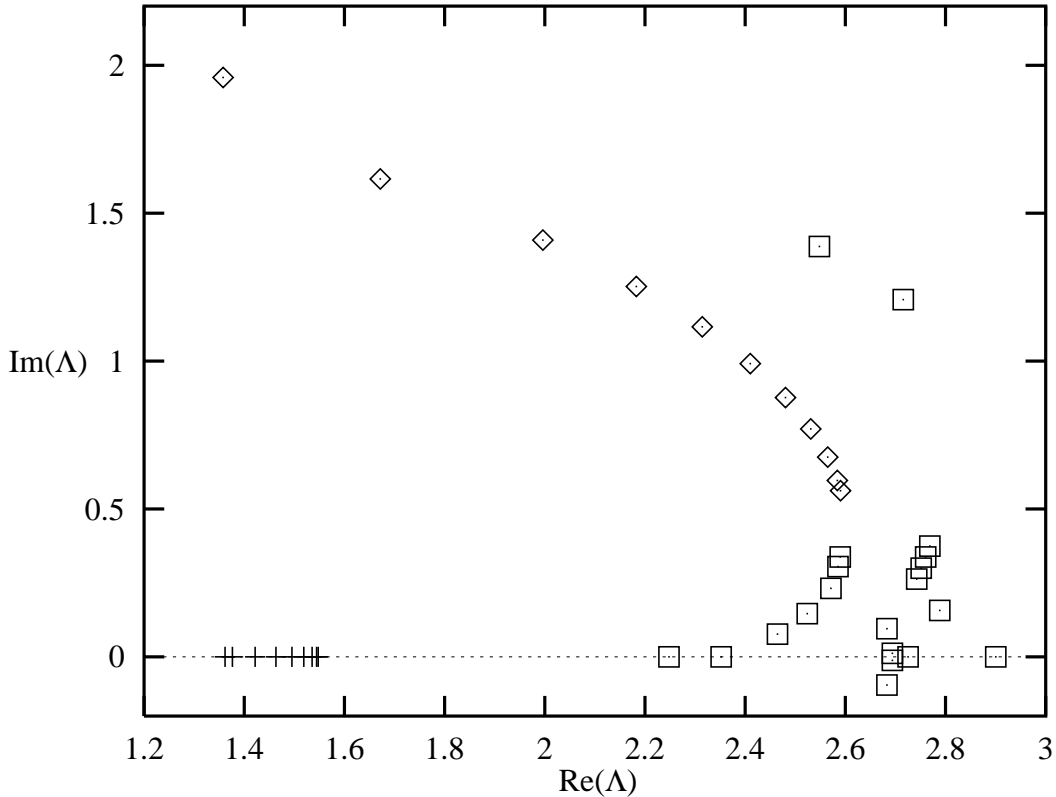


**Fig. 4:** Eigenvalues of the forest-fire Hamiltonian with  $L = 20$  sites,  $p = 1$ ,  $f = 0.1$ . For the symbols compare the text.

The comparably large value of  $f = 0.1$  has been chosen in order to have the dispersionless modes (3.15) separated from the low-lying part of the spectrum. The first one of these modes is located at  $\Lambda = 2.9$  in Fig. 4. One observes a group of levels on the real axis indicated by the symbols ‘+’. The level with the smallest gap has  $P = 4\pi/L$ . Then the gap increases with increasing  $P$  and reaches its maximum at  $P = \pi$ . One can also clearly see another sequence of complex-conjugate levels (which are drawn with the symbol ‘◇’) starting around  $\Lambda = 1.4 \pm 2i$  for  $P = 0$  and tending to  $\Lambda = 2.6 \pm 0.56i$  for  $P \rightarrow \pi$ . There are also further levels in this region. The ones we have computed are marked by the symbol ‘□’ in Fig. 4. They do not form groups as clearly as the levels described before. It is also possible that some of them will still move considerably with increasing  $L$  due to their interaction with the mode at  $\Lambda = 1 + f(L - 1)$ .

The levels drawn with the symbols ‘+’ and ‘◇’ are isolated levels for fixed  $P$  and remind one of dispersion curves for fundamental particle states. However, single-particle states usually have exponentially small corrections in the chain length, whereas the levels under consideration have larger corrections (compare also below). This and the behaviour of the dispersion relations as a function of  $P$  around  $P = 0$  respective  $P = \pi$  makes an interpretation as fundamental particle states of these levels not very plausible. Neither can we see multi-particle states whose scattering bands would form continua, i.e. the levels

in Fig. 4 would have to group more densely for  $P$  fixed. Even if the levels corresponding to the symbols ‘+’ and ‘◇’ were considered as fundamental single-particle states, some of the remaining levels which we denoted by ‘□’ would remain unexplained. Thus, the figure demonstrates that the relaxational spectrum of the Hamiltonian (3.6) does not have a simple particle interpretation.

In the remainder of this section we concentrate on the behaviour of the lowest gap  $\Lambda_{\text{ex}}$  in the translationally invariant sector. In Fig. 4 one has  $\Lambda_{\text{ex}} \approx 1.3579 \pm 1.9586i$ . Whether the level  $\Lambda_{\text{ex}}$  actually has the smallest real part, or if other levels exhibit different critical behaviour would require more detailed investigations which are beyond the scope of the present paper. The restriction to  $P = 0$  is convenient because only in the translationally invariant sector the finite-size effects can be analyzed easily. In addition, measurements involving spatial averages project onto this sector, so that it plays a particular rôle.

Table 1 contains asymptotic values obtained numerically for the gap  $\Lambda_{\text{ex}}$ . They were obtained by computing numerically the lowest complex conjugate levels <sup>1)</sup> for  $5 \leq L \leq 20$  and extrapolating to  $L = \infty$  using the van den Broeck-Schwartz algorithm (see e.g. [24]).

	diagonalization ( $p = 1$ )		simulation with $p = 1/200$ , $L = 10000$	
$f/p$	$\lim_{L \rightarrow \infty} \Lambda_{\text{ex}}$	error of $ \lim_{L \rightarrow \infty} \Lambda_{\text{ex}} $	relaxation time	oscillation period
0.1	$1.2947 \pm 2.0030i$	0.0003	140	560
0.09	$1.2344 \pm 1.9625i$	0.0003	150	575
0.08	$1.1726 \pm 1.9170i$	0.0002	160	615
0.07	$1.1069 \pm 1.8664i$	0.0002	160	695
0.06	$1.0360 \pm 1.8093i$	0.0004	190	705
0.05	$0.9600 \pm 1.7461i$	0.0004	205	715
0.04	$0.8767 \pm 1.6721i$	0.0003	255	740
0.03	$0.7820 \pm 1.5820i$	0.0010	270	775
0.02	$0.6780 \pm 1.4680i$	0.0040	300	875

Table 1: Estimates for the first translationally invariant gap of the forest-fire Hamiltonian.

The values in table 1 have to be considered with some care because the maximal system size  $L = 20$  used for the extrapolation to  $L = \infty$  is still quite small. However, all sequences used for the extrapolation are monotonic in  $L$ . Furthermore, the deviation at finite  $L$  from the values given above is typically of the order  $L^{-2}$ . Under these conditions one can usually obtain reliable estimates for the thermodynamic limit  $L = \infty$  although the estimates in table 1 for the error of  $\Lambda_{\text{ex}}$  may be somewhat too optimistic.

In order to perform a further check of the extrapolations we have simulated the temporal behaviour of the average density of trees  $\rho(t)$ . This quantity approaches its limiting value  $\rho(\infty)$  in an oscillatory way. The simulations were performed for  $p = 1/200$  on a lattice of size  $L = 10000$  – a size that is much closer to the thermodynamic limit. For one random initial condition with  $\rho(0) = \frac{1}{2}$  the time evolution of  $\rho(t)$  was averaged over 100 realizations.

<sup>1)</sup> Typically these levels fall below others (with respect to the real part), which are located on the real axis, for  $L \sim 10$  in the range of  $f$  considered here.

Then the oscillation period was determined by looking for crossings of  $\rho(t)$  at early times  $t$  with the stationary value  $\rho(\infty)$  (which can be estimated from  $\rho(t)$  for large  $t$ ). The relaxation time can be obtained by looking at the values of local extrema of  $\rho(t)$  at early times. If only one complex pair contributes, the relaxation time equals  $1/(p \operatorname{Re}(\Lambda_{\text{ex}}))$  while the oscillation period is given by  $2\pi/(p \operatorname{Im}(\Lambda_{\text{ex}}))$ , where  $\Lambda_{\text{ex}}$  is the normalized relaxational mode at  $p = 1$ . One obtains good agreement with the extrapolations in Table 1 keeping the crude method in mind which can at most be expected to be accurate to 10%.

Because the extrapolations can be performed much more accurately we used them in order to determine the behaviour of  $\Lambda_{\text{ex}}$  as a function of  $f$ . The data in Table 1 can nicely be fitted by

$$\lim_{L \rightarrow \infty} \Lambda_{\text{ex}} = 3.258 f^{0.405} \pm 3.127i f^{0.194}. \quad (4.1)$$

This is consistent with a standard critical point at  $f = 0$  – like the simulations of the correlation functions in Section 2. We would like to point out that this critical behaviour arises because the limits  $f \rightarrow 0$  and  $L \rightarrow \infty$  do not commute. Taking  $f \rightarrow 0$  first, one has  $\Lambda_{\text{ex}} = 1$  for all  $L$ .

The critical exponents in (4.1) may still have systematic errors due to the fact that only systems of maximal size  $L = 20$  were used and that because of this restriction in the system size we could not get closer to the critical point than  $f = 0.02$ . Thus, the critical exponents for the oscillation frequency  $\operatorname{Im}(\Lambda_{\text{ex}})$  and inverse relaxation time  $\operatorname{Re}(\Lambda_{\text{ex}})$  could be  $1/5$  and  $2/5$ , respectively.

## 5. Simplified models in the symmetric space

---

In this section we consider several simplified models that deal only with the total number of trees respectively empty places. The main motivation is that the critical correlation functions (3.13) follow most easily from such a simplified model. Because this simplified model exhibits neither the critical behaviour (2.8) nor the gap (4.1) we investigate whether it is possible to generalize the model in the symmetric space such that it describes also some aspects off the critical point correctly. It turns out that the natural generalizations do not have these properties. This shows that most of the critical exponents of the ffm seem to be due to actual correlations while the power laws of the critical correlation functions (3.13) are a global effect.

The first simplified model corresponds to the first-order expansion (3.10). It consists in modifying the dynamics in such a way that this first-order expansion of the ground state becomes exact. Since only the burning of the completely full system contributes in first-order perturbation theory, this is achieved by dropping all lightning processes except for the completely full system (see also [16]). This modification leaves the space of states (3.8) invariant, so one can restrict oneself to this subspace. We call it symmetric since the states are invariant under permutations of the lattice sites. Consequently, there is no real spatial structure for this simplified model any more.

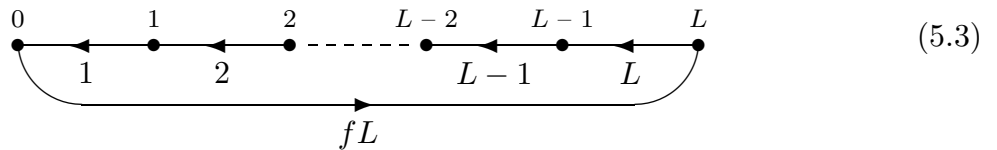
It is useful to replace the basis (3.8) by the following differently normalized one:

$$|\tilde{N}\rangle := \frac{|N\rangle}{\binom{L}{N}}. \quad (5.1)$$

The normalization factor in (5.1) is precisely the number of configurations contributing to  $|N\rangle$ . In this basis the simplified Hamiltonian is given by the following  $(L + 1) \times (L + 1)$  matrix:

$$H_s = \begin{pmatrix} fL & -1 & 0 & \cdots & 0 \\ 0 & 1 & -2 & \ddots & \vdots \\ \vdots & \ddots & 2 & \ddots & 0 \\ 0 & & \ddots & \ddots & -L \\ -fL & 0 & \cdots & 0 & L \end{pmatrix}. \quad (5.2)$$

The normalization of the states in (5.1) is chosen such that the Hamiltonian (5.2) is a manifestly stochastic one, i.e. the columns sum to zero. It describes a single particle hopping on a ring with sites  $0, \dots, L$  with the following rates:



By construction, the state (3.10) is the exact ground state of the simplified Hamiltonian (5.2). In the basis (5.1) it reads

$$|G\rangle = |\tilde{0}\rangle + fL \sum_{N=1}^L \frac{1}{N} |\tilde{N}\rangle. \quad (5.4)$$

One can use this simplified model to obtain the result (3.13). The equation of motion for the quantity  $n_r(s)$  (see (3.12)) is:

$$\partial_t n_r(s) = -(r+1)n_r(s) + sn_{r+1}(s-1) \quad (5.5)$$

for  $0 < s < L$ ,  $r \geq 0$ . The first term describes the loss term by tree growth at any of the  $r+1$  empty places whereas the second term is the gain term by a tree having grown at any of the  $s$  places that are occupied by trees in the final configuration. Note that lightnings affect only configurations with  $s=0$  or  $s=L$  trees and are therefore not relevant for the present consideration. In the stationary state, eq. (5.5) leads to the recurrence relation  $n_{r+1}(s-1) = (r+1)n_r(s)/s$ . Together with the combinatorial proof of (3.13) for  $r=0$  presented in appendix A this proves (3.13) for general  $r$ .

Now we proceed with a discussion of the excitation spectrum of  $H_s$ . The characteristic polynomial of  $H_s$  yields the equation

$$(fL - \lambda) \prod_{r=1}^L (r - \lambda) - fL \prod_{r=1}^L r = 0 \quad (5.6)$$

for the eigenvalues  $\lambda$ . A discussion of this characteristic polynomial leads to the following results on the relaxational spectrum

$$\text{Im}(\lambda_k) = \frac{2\pi k}{\ln(L)}, \quad k \in \mathbb{Z}, \quad \text{Re}(\lambda_1) = \frac{\pi^4}{3 \ln(L)^3} \quad (5.7)$$

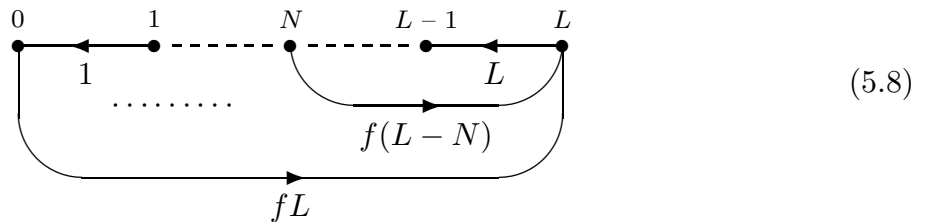


for  $L$  large. A numerical computation of the lowest eigenvalues of  $H_s$  up to  $L \approx 10^3$  yields good agreement with the result (5.7) for  $\text{Im}(\lambda_k)$ . The precise behaviour of the real part is more difficult to verify, but from the numerical computations one sees that the real parts of at least the lowest eigenvalues tend much faster to zero than their imaginary parts.

The result for  $\text{Im}(\lambda)$ , as well as the eigenfunctions can also be obtained from a continuum approximation. Details of the computation are presented in appendix C. The continuum model shows that the eigenfunctions are essentially plane waves in the variable  $\ln(N)/\ln(L)$  multiplied by  $1/N$ . In this variable, the  $k$ th eigenfunction has  $k$  periods. Therefore, the value  $1/\text{Im}(\lambda_k)$  can be interpreted as the average time that a particle needs to hop around the  $k$ th part (on this logarithmic scale) of the chain.

In summary, the gap of the simplified Hamiltonian (5.2) vanishes as  $1/\ln(L)$  as  $L \rightarrow \infty$  irrespective of the value of  $f$ <sup>2)</sup>. This is different from the behaviour of the full ffm as observed in the previous section.

The simplified model (5.2) discussed so far is not able to describe the behaviour of the full ffm away from the critical point. As a first step in this direction one can take all loss terms due to lightning in the full model into account. In order to have a stochastic process these loss terms must be balanced with suitable gain terms. A convenient choice is to attribute all gain terms to the completely empty system. Thus, in this generalization of (5.2) we introduce transitions from the state  $|\tilde{N}\rangle$  to the state  $|\tilde{L}\rangle$  with weight  $f(L - N)$ . Then the picture (5.3) turns into:



It is straightforward to obtain the ground state of the Hamiltonian corresponding to (5.8) either numerically up to  $L \approx 10^4$ , or from a continuum approximation. Then one finds for the cluster-size distribution

$$n(s) \sim s^{-(2+fL)} \quad (5.9)$$

for  $s \gg 1$ . It is tempting to interpret this result as a continuously varying critical exponent but then one has to introduce a rescaled rate  $\hat{f} = fL$  in order to keep the exponent finite in the thermodynamic limit. In any case, the loss processes by lightning strokes in (5.8) do not account for the finite correlation length  $\xi_c$ . This is surprising because consideration of the same processes (with some additional approximations) lead to the correct critical behaviour (2.8) of the correlation length  $\xi_c$  [13]. A solution to this puzzle might be the following: Once one assumes that there is an upper cutoff, the loss processes by lightning strokes fix its critical exponent although these processes alone do not explain the presence of this cutoff.

---

<sup>2)</sup> The logarithmic dependence of the relaxation time on the system size is reminiscent of results obtained in [25] for certain two-dimensional kinetic spin models with cluster dynamics.

Other possible modifications of the simplified Hamiltonian  $H_s$  are:

- 1) One can introduce death of trees irrespective of their neighbourhood with a rate  $q$ , thereby modeling the ignition processes which dominate in the full model if the number of trees is small. For  $f = 0$  one then has a simple kinetic model where the spins flip independently and  $n(s)$  varies exponentially with  $s$ . However, this does not give an upper cutoff in the general case since then  $n(s)$  is well approximated by a *sum* of the results for  $f = 0$  and  $q = 0$ , respectively.
- 2) One can distribute the loss terms in (5.8) equally over the configurations with fewer trees. This amounts to introducing a transition from a state  $|\widetilde{N}_i\rangle$  to a state  $|\widetilde{N}_f\rangle$  for  $N_f > N_i$  with rate  $f$ . Computing the ground state numerically as before, one finds that this model behaves very similarly to that in (5.8). In particular, its cluster-size distribution also has the behaviour (5.9).

Since none of the aforementioned models is able to describe the off-critical behaviour correctly, let us finally discuss the accurate projection of the full  $\text{ffm}$  onto the symmetric subspace. This projection can be performed as follows: Consider the matrix element of  $V$  that leads from  $N_i$  empty places to  $N_f$  empty places, i.e. a cluster of  $N_f - N_i$  trees is struck by lightning. Thus, there must have been  $L - N_f$  trees outside the cluster in the initial state. This cluster occupies  $2 + N_f - N_i$  places including the two empty places at its boundary. This leads to a combinatorial factor  $\binom{L-2-N_f+N_i}{L-N_f}$  in the transition matrix element. Translational invariance yields another factor  $L$  and the weight for the process is  $N_f - N_i$ . Writing this in the normalization (5.1) leads to the matrix element

$$\langle \widetilde{N}_f | V | \widetilde{N}_i \rangle = \frac{L (N_f - N_i) \binom{L-2-N_f+N_i}{L-N_f}}{\binom{L}{N_i}} \quad (5.10)$$

for  $N_f > N_i$ . The loss term due to lightning equals  $\langle \widetilde{N} | V | \widetilde{N} \rangle = -(L - N)$  and  $\langle \widetilde{N}_f | V | \widetilde{N}_i \rangle = 0$  for  $N_f < N_i$ . The tree growth has already been correctly accounted for in (5.2). Putting this together, one obtains the correct projection of the full Hamiltonian (3.6) onto the symmetric subspace. The corresponding matrix is almost triangular.

As for the other simplified models, the ground state and thus the cluster-size distribution of this Hamiltonian can easily be obtained from a numerical diagonalization for rings with up to a few thousands sites. For small  $f$  one finds again  $n(s) \sim s^{-(2+fL)}$  for  $s \gg 1$  and *no* crossover to an exponential decay. For  $f$  large,  $n(s)$  decays rapidly already for small  $s$ . In this case, the  $L$ -dependence of  $n(s)$  computed in the symmetric subspace for small  $s$  becomes small and one can even observe qualitative agreement with simulations of the full model. However, even in the case (5.10) the critical behaviour (2.8) for  $f \rightarrow 0$  is not reproduced. In summary, the symmetric space seems unable to describe the critical behaviour as a function of  $f$ , while it does describe the critical correlation functions (3.13) very nicely.

## 6. Discussion

---

In this paper we have studied the one-dimensional forest-fire model and exhibited several new non-integral critical exponents. It remains to be seen to what extent our results are relevant for higher dimensions as well. Firstly, it should be checked to a better accuracy whether  $\nu = \nu_T$  [14] is indeed true in two dimensions. Another question to be addressed is if in higher dimensions the spatial power laws associated with clusters can also be obtained by looking at global quantities only. In particular, it remains an open problem if models in a symmetric subspace can also describe the critical cluster-size distribution in higher dimensions. The two-dimensional version of the ffm introduced in [26] seems to point in this direction. In this case, the dynamics is also controlled by a global quantity, namely the mean density of trees.

The fact that the critical density in one dimension is  $\rho = 1$  leads to the unusual situation that all correlation functions at the critical point become independent of the spatial variables in the thermodynamic limit. At  $f = 0$ , the density in the stationary state equals one for all dimensions. Now, a necessary requirement for perturbation theory around  $f = 0$  to be of any use is that the density  $\rho$  must be continuous for  $f \rightarrow 0$ . In one dimension, this condition is satisfied, which permitted us to employ perturbation theory and thus led to the simplified model. The situation is different in higher dimensions where the critical density is smaller than one. Then correlation functions with non-trivial spatial behaviour at the critical point are possible, but perturbation theory around  $f = 0$  cannot be used.

Even if at present our results seem to be specific for one dimension, our simple model in the symmetric space shows that spatial power laws can arise from purely global effects. A similar observation for certain models of evolution was made recently in [17] where the impact of replacing local neighbourhoods by random neighbourhoods was examined. In our case, this global dynamics arises naturally at the critical point and is not put in by hand. We have also shown that this simplified model has a vanishing gap, i.e. physical quantities will relax with a temporal power law to the stationary state. This demonstrates that neither power laws in static quantities related to avalanche type processes nor slow relaxational modes are a sufficient criterion for criticality in a strict sense, so that the usual multi-point correlations should always be studied in addition.

## Acknowledgments

---

We thank B. Drossel, M. Kaulke and F. Schwabl for discussions and comments. A.H. would like to thank the Deutsche Forschungsgemeinschaft for financial support.

## Appendix A. A combinatorial identity

---

We want to show that

$$S(L, s) := \sum_{N=1}^{L-s} \frac{\binom{L-s-1}{N-1}}{\binom{L-1}{N-1}} = \frac{L}{s+1} \quad (\text{A.1})$$

for  $0 \leq s \leq L-1$ . The proof uses induction on  $L$ . First one observes that

$$S(L, L-1) = 1 \quad (\text{A.2})$$

which gives the start of the induction. Now one can proceed with the following induction step

$$S(L+1, s) = \sum_{N=1}^{L+1-s} \prod_{u=0}^{s-1} \frac{L+1-N-u}{L-u} = 1 + \frac{L-s}{L} S(L, s). \quad (\text{A.3})$$

Observing that the r.h.s. of (A.1) satisfies the recurrence relation (A.3) completes the proof of this combinatorial identity.

## Appendix B. Perturbation expansion for excitations

---

In this appendix we indicate how to compute the excitation spectrum of the ffm using quantum-mechanical perturbation theory. First we note that  $H_0$  in (3.6) can easily be diagonalized. In matrix form the part at one site is given by

$$(H_0)_x = \begin{pmatrix} 0 & -1 \\ 0 & 1 \end{pmatrix}. \quad (\text{B.1})$$

The right eigenvectors of this matrix are

$$\begin{pmatrix} 1 \\ 0 \end{pmatrix}, \quad \begin{pmatrix} -1 \\ 1 \end{pmatrix} \quad (\text{B.2})$$

with eigenvalues 0 and 1, respectively. The corresponding left eigenvectors are

$$(11), \quad (01). \quad (\text{B.3})$$

Now one can treat excited states with standard quantum-mechanical perturbation theory where one just has to keep in mind that the left eigenvectors (B.3) are not just the transposed ones of the right eigenvectors (B.2). From (B.2) and (B.3) it follows immediately that the right vectors

$$|x\rangle = -|1\dots 1\rangle + |1\dots 1 \underset{x}{0} 1\dots 1\rangle \quad (\text{B.4})$$

and the left vectors

$$\langle y| = \sum_{i_1, i_2, \dots = 0}^1 \langle i_1 i_2 \dots \underset{y}{0} \dots | \quad (\text{B.5})$$

are eigenvectors of  $H_0$  with eigenvalue 1. The normalization in (B.4) and (B.5) is already  $\langle y|x\rangle = \delta_{y,x}$ . Now one easily checks that

$$\langle y|V|x\rangle = \left[ \begin{pmatrix} L-1 & & \\ & \ddots & \\ & & L-1 \end{pmatrix} + \begin{pmatrix} 1 & \cdots & 1 \\ \vdots & & \vdots \\ 1 & \cdots & 1 \end{pmatrix} \right]_{yx}. \quad (\text{B.6})$$

The eigenvalues of the matrix (B.6) are straightforward to compute. The result is that  $H$  has one eigenvalue  $1 + f(2L - 1) + \mathcal{O}(f^2)$  and  $(L - 1)$  degenerate eigenvalues  $1 + f(L - 1) + \mathcal{O}(f^2)$ . The latter correspond to the result (3.15) for  $P \neq 0$ , and in this case the first-order expansion happens to be exact for all  $f > 0$ . The new result of the perturbation expansion is the eigenvalue  $1 + f(2L - 1) + \mathcal{O}(f^2)$  which is located in the sector  $P = 0$ .

Similarly, one finds that the  $L(L - 1)/2$  vectors

$$|x_1, x_2\rangle = |1 \dots 1\rangle - |\dots 1 \underset{x_1}{0} 1 \dots\rangle - |\dots 1 \underset{x_2}{0} 1 \dots\rangle + |\dots 1 \underset{x_1}{0} 1 \dots 1 \underset{x_2}{0} 1 \dots\rangle \quad (\text{B.7})$$

with  $x_1 < x_2$  are right eigenvectors of  $H_0$  with eigenvalue 2. The corresponding left eigenvectors are given by

$$\langle y_1, y_2 | = \sum_{i_1, i_2, \dots = 0}^1 \langle i_1 i_2 \dots \underset{y_1}{0} \dots \underset{y_2}{0} \dots | \quad (\text{B.8})$$

with  $y_1 < y_2$ . These vectors are properly normalized, i.e.  $\langle y_1, y_2 | x_1, x_2 \rangle = \delta_{y_1, x_1} \delta_{y_2, x_2}$ . A straightforward computation yields

$$\langle y_1, y_2 | V | x_1, x_2 \rangle = (L-2)(1 + \delta_{y_1, x_1} \delta_{y_2, x_2}) - \begin{cases} (x_2 - x_1 - 1) & \text{if } x_1 \leq y_1, y_2 \leq x_2 \\ (L - x_2 + x_1 - 1) & \text{if } \begin{cases} y_1 \leq x_1, x_2 \leq y_2 \\ \text{or } x_2 \leq y_1 \\ \text{or } y_2 \leq x_1 \end{cases} \\ 0 & \text{otherwise.} \end{cases} \quad (\text{B.9})$$

It is easy to check that the  $L$  vectors  $|x, x + 1\rangle$  are eigenvectors of (B.9) with eigenvalue  $(L - 2)$ . In particular, there is an eigenvalue  $2 + f(L - 2) + \mathcal{O}(f^2)$  of  $H$  for each momentum (including the translationally invariant sector) which is compatible with the result (3.15) for  $P \neq 0$ .

All first-order corrections discussed so far are positive, but the matrix (B.9) also has negative eigenvalues. Since the eigenvalues of a stochastic matrix always have positive real parts, this automatically implies that such a negative correction can only be relevant for small  $f$ . More precisely, one finds eigenvalues  $2 - fh(L, P) + \mathcal{O}(f^2)$  where  $h(L, P)$  is positive around  $P = \pi$ , symmetric in  $P - \pi$  and increases for small  $|P - \pi|$ . This does however not affect the translationally invariant sector, nor is it relevant for the large  $L$  limit. Nevertheless, the complicated  $P$ -dependence of these modes demonstrates that the structure of the full relaxation spectrum is highly non-trivial.

## Appendix C. Continuum approximation

---

The model described by  $H_s$  in section 5 can be treated in the following continuum approximation which gives the imaginary part of the spectrum and the eigenfunctions in a simple way.

Denote the eigenvalues by  $\lambda$  and the components of the corresponding eigenvector by  $g_0, \dots, g_L$ . Then the eigenvalue problem for (5.2) is given by the following equations:

$$fLg_0 - g_1 = \lambda g_0, \quad (\text{C.1a})$$

$$Ng_N - (N+1)g_{N+1} = \lambda g_N, \quad 1 < N < L, \quad (\text{C.1b})$$

$$-fLg_0 + Lg_L = \lambda g_L. \quad (\text{C.1c})$$

The solution of the inner equations  $-(N+1)(g_{N+1} - g_N) - g_N = \lambda g_N$  varies only slowly for large  $N$  so that we can approximate them by

$$-x \frac{d}{dx} g(x) = (\lambda + 1)g(x) \quad (\text{C.2})$$

for  $1 \leq x \leq L$ . Keeping only the leading term in  $L$  of the boundary conditions (C.1a), (C.1c) and eliminating  $g_0$  one finds

$$g(L) = \frac{g(1)}{L}. \quad (\text{C.3})$$

For the stationary state these equations lead to  $g(x) = 1/x$  which corresponds exactly to the discrete result  $g_N \sim 1/N$ .

The general solution of the differential equation (C.2) is given by

$$g(x) = x^{-(\lambda+1)} \quad (\text{C.4})$$

and from the boundary condition (C.3) one finds the purely imaginary spectrum

$$\lambda_k = \frac{2\pi ik}{\ln(L)}, \quad k \in \mathbb{Z}. \quad (\text{C.5})$$

The eigenfunctions are plane waves in the variable  $\ln(x)/\ln(L)$  multiplied by  $1/x$  and compare well with those of the discrete problem (C.1), except for small  $x$ .

## References

---

- [1] P. Bak, C. Tang, K. Wiesenfeld, *Self-Organized Criticality: An Explanation of  $1/f$  Noise*, Phys. Rev. Lett. **59** (1987) 381-384
- [2] P. Bak, C. Tang, K. Wiesenfeld, *Self-Organized Criticality*, Phys Rev. **A38** (1988) 364-374
- [3] P. Bak, K. Chen, C. Tang, *A Forest-Fire Model and Some Thoughts on Turbulence*, Phys. Lett. **A147** (1990) 297-300
- [4] P. Bak, K. Sneppen, *Punctuated Equilibrium and Criticality in a Simple Model of Evolution*, Phys. Rev. Lett. **71** (1993) 4083-4086
- [5] P. Bak, H. Flyvbjerg, K. Sneppen, *Mean Field Theory for a Simple Model of Evolution*, Phys. Rev. Lett. **71** (1993) 4087-4090
- [6] P. Grassberger, H. Kantz, *On a Forest Fire Model with Supposed Self-Organized Criticality*, J. Stat. Phys. **63** (1991) 685-700
- [7] B. Drossel, W.K. Moßner, F. Schwabl, *Computer Simulations of the Forest-Fire Model*, Physica **A190** (1992) 205-217
- [8] B. Drossel, F. Schwabl, *Self-Organized Critical Forest-Fire Model*, Phys. Rev. Lett. **69** (1992) 1629-1632
- [9] V. Loreto, L. Pietronero, A. Vespignani, S. Zapperi, *Renormalization Group Approach to the Critical Behavior of the Forest Fire Model*, Phys. Rev. Lett. **75** (1995) 465-468
- [10] B. Drossel, F. Schwabl, *Self Organization in a Forest-Fire Model*, Fractals **1** (1993) 1022-1029
- [11] S. Clar, B. Drossel, F. Schwabl, *Scaling Laws and Simulation Results for the Self-Organized Critical Forest-Fire Model*, Phys. Rev. **E50** (1994) 1009-1018
- [12] P. Bak, M. Paczuski, *Theory of the One-Dimensional Forest-Fire Model*, Phys. Rev. **E48** (1993) R3214-R3216
- [13] S. Clar, B. Drossel, F. Schwabl, *Exact Results for the One-Dimensional Self-Organized Critical Forest-Fire Model*, Phys. Rev. Lett. **71** (1993) 3739-3742
- [14] C.L. Henley, *Statics of a "Self-Organized" Percolation Model*, Phys. Rev. Lett. **71** (1993) 2741-2744
- [15] F.C. Alcaraz, M. Droz, M. Henkel, V. Rittenberg, *Reaction-Diffusion Processes, Critical Dynamics, and Quantum Chains*, Ann. Phys. **230** (1994) 250-302
- [16] S. Clar, B. Drossel, F. Schwabl, *Universality in the One-Dimensional Self-Organized Critical Forest-Fire Model*, Z. Naturforsch. **49** (1994) 856-860
- [17] J. de Boer, A.D. Jackson, T. Wettig, *Criticality in Simple Models of Evolution*, Phys. Rev. **E51** (1995) 1059-1074
- [18] P. Grassberger, *On a Self-Organized Critical Forest-Fire Model*, J. Phys. A: Math. Gen. **26** (1993) 2081-2089
- [19] F.Y. Wu, *The Potts Model*, Rev. Mod. Phys. **54** (1982) 235-268
- [20] G. Grinstein, C. Jayaprakash, J.E.S. Socolar, *On Self-Organized Criticality in Non-conserving Systems*, Phys. Rev. **E47** (1993) 2366-2376
- [21] B. Drossel, *Strukturbildung in offenen Systemen*, Ph.D. thesis, München (1994)
- [22] H. Patzlaff, S. Trimper, *Analytical Approach to the Forest-Fire Model*, Phys. Lett. **A189** (1994) 187-192
- [23] S. Bottani, B. Delamotte, *Towards a Field Theory Analysis of Self-Organized Criticality: The Forest Fire and Sandpile Models*, LP THE preprint 95/10

- [24] M. Henkel, G.M. Schütz, *Finite-Lattice Extrapolation Algorithms*, J. Phys. A: Math. Gen. **21** (1988) 2617-2633
- [25] A.N. Burkitt, D.W. Heermann, *System Size Dependence of the Autocorrelation Time for the Swendsen-Wang Ising Model*, Physica **A162** (1990) 210-214
- [26] S. Clar, B. Drossel, F. Schwabl, *Self-Organized Critical and Synchronized States in a Nonequilibrium Percolation Model*, Phys. Rev. Lett. **75** (1995) 2722-2725